Shear Behavior Study on Timber-Concrete Composite Structures with Bolts

Guojing He,[a] Lan Xie,[a,*] Xiaodong (Alice) Wang,[b] Jin Yi,[a] Lening Peng,[a] Zi'ang Chen,[a] Per Johan Gustafsson,[c] and Roberto Crocetti [c]

The key point of design for timber-concrete composite structure is to ensure the reliability of shear connectors. This study examined the mechanical properties of bolt-type connectors in timber-concrete composite structures theoretically and experimentally. The theoretical study was based on the Johansen yield theory (European Yield Model). Push-out specimens with different bolt dimensions were tested to determine the shear capacity and slip modulus. According to the experimental results, bolts yielded without timber or concrete cracks when the stiffness of bolts was not very great. The shear capacity and slip modulus of the bolt connectors were directly proportional to the diameter of the bolt. The strength of concrete was found to significantly affect the shear capacity of bolt connectors. Comparison between the theoretical and the experimental shear strength results showed reasonable agreement.

Keywords: Timber-concrete composite structure; Bolt connectors; Mechanical model; Shear capacity equation; Push-out tests; Slip modulus

Contact information: a: Department of Civil Engineering and Mechanics, Central South University of Forestry and Technology, 498 Shaoshan Road, Changsha, Hunan, 410004 China; b: Wood Technology and Engineering, Luleå University of Technology, Forskargatan 1, SE-931 87 Skellefteå, Sweden; c: Division of Structural Mechanics, Lund University, Box 188, 221 00 Lund, Sweden;
** Corresponding author: lily.csuft.xie@gmail.com; xieyuantaixielan@126.com*

INTRODUCTION

Timber-concrete composite structures have been utilized in Europe over the past 50 years, especially in new buildings (Natterer *et al.* 1996) and in the upgrading of existing timber floors. A timber-concrete composite (TCC) structure contains a concrete slab and a timber joist. The upper concrete flange and timber joist may be connected with various kinds of shear connectors. In this case, the concrete bears compression force, while the timber fiber is in tension. The TCC structure brings the superiority of those two materials into full play. TCC structures are strong and stiff, and thus perform well in dead load, earthquake, and fire (Skinner *et al.* 2014). In contrast to concrete structures, TCC structures are highly energy efficient and can significantly reduce CO_2 emissions through a carbon sequestration mechanism, as timber is a carbon store (Rodrigues *et al.* 2013). These features are the advantages of timber-concrete composite structure (Lukaszewska 2009). In China, the importance of environmental protection is increasingly realized and the use of TCC will probably become extensive also in China.

Notably, it is important to use connectors that are strong and stiff enough to resist the shear force in the composite structure (Yeoh *et al.* 2011). Various kinds of connectors have been developed, including screw or stud connectors, dowels, and notches cut in the timber and filled with concrete. Mascia and Soriano (2004) studied the properties of TCC

push-out specimens and beams with nails or screws. Dias *et al.* (2010) analyzed the experimental and numerical assessment of the stiffness of timber–concrete joints, made with dowel-type fasteners. Dias *et al.* (2007) analyzed the load-carrying capacity of timber–concrete joints made with dowel-type fasteners. Van de Kuilen and Dias (2011) discussed the long-term mechanical behaviour of timber-to-concrete joints made with dowel-type fasteners. There has been experimental research on TCC structures (Grantham *et al.* 2004; Clouston *et al.* 2005), but a suitable theoretical equation has not been given. Additionally, there has been little research on TCC in China, and the available literature and code in Europe and north America should be verified to guide the design of TCC using Chinese timber.

This study investigated the mechanical properties of bolt-type connectors in TCC push-out specimens theoretically and experimentally. Based on the Johansen yield theory (Johansen 1962), three failure modes were presented, and the shear capacity of bolt-type connectors was studied. The load-slip curves of these specimens were used to analyze the connector property of TCC structures with interlamination slips. Additionally, TCC push-out components with different bolt parameters were studied to predicate the failure mode and mechanical property of the connector.

EXPERIMENTAL

Mechanics-based Shear Capacity Equation

A TCC structure will fail if any component fails. But it mainly fails because of failure of a connection. In accordance with the Johansen yield theory (Johansen 1962), the possible failure modes are presented in Fig. 1. The equilibrium expressions (Eqs. 1 to 12), corresponding to situations in which there was a balance of forces or moment, were obtained according to the failure modes.

In Fig. 1 a), at a plastic hinge, the shear force is zero (Li *et al.* 2014), and the bending moment has its maximum value, M_y. The diameter of the bolt in Fig. 1 a) was denoted as d, and the stresses acting on the bolt in timber and concrete were assumed as reaching the embedment strength, $f_{h,t}$ and $f_{h,c}$, respectively. Thus, the equilibrium is written as,

$$f_{h,t} d b_1 = f_{h,c} d b_2 = \beta f_{h,t} d b_2 \quad (1)$$

where $f_{h,t}$ =embedment strength in timber; $f_{h,c}$ = embedment strength in concrete; d =diameter of bolt; b_1=distance between plastic hinge in timber and timber edge; b_2 = distance between concrete edge and plastic hinge in concrete; β =ratio of embedment strength in concrete and in timber (see Eq. 2).

$$\beta = \frac{f_{h,c}}{f_{h,t}} \quad (2)$$

The moment equilibrium at the yielding point of bolts in timber is determined by,

$$2M_y = -f_{h,t} d \frac{b_1^2}{2} + f_{h,c} d b_2 (b_1 + \frac{b_2}{2}) \quad (3)$$

where M_y =yield moment of bolt, other variables are the same as Eq. (1) and Eq. (2).

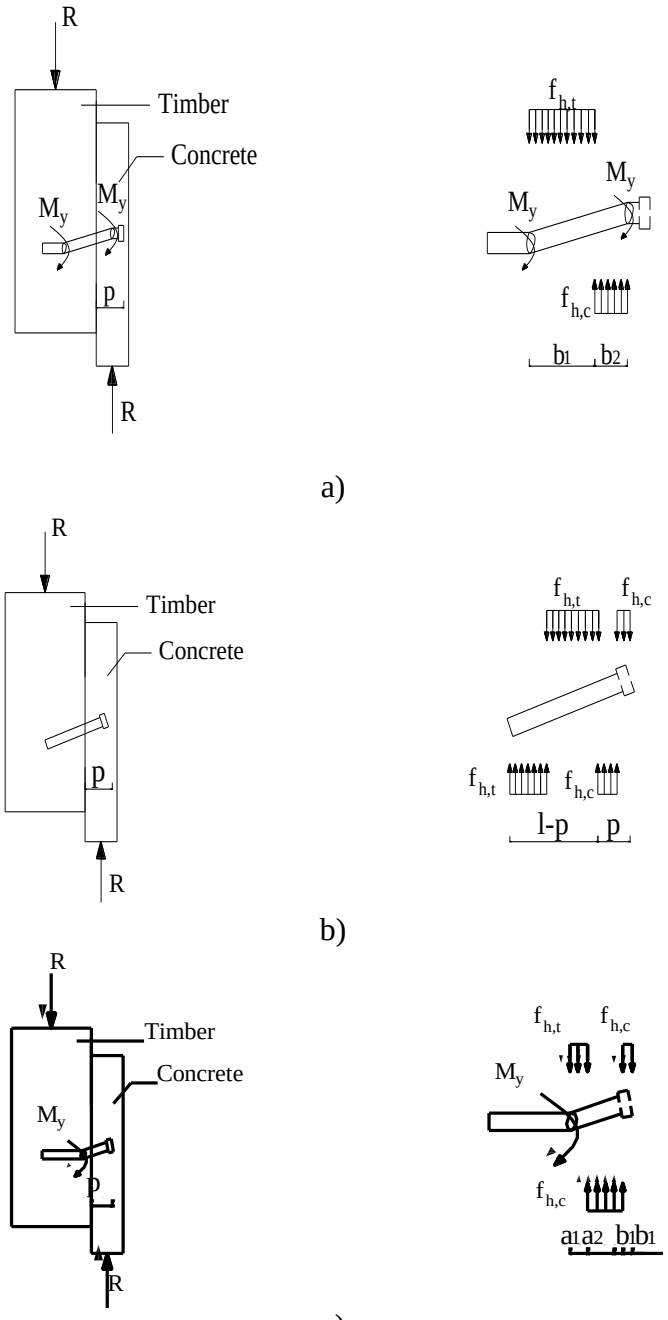

Fig. 1. Mechanism of bolt-type connector failure: a) failure mode with two plastic hinges, b) failure mode with rotation, c) failure mode with one plastic hinge

Eq. 1 gives $b_1 = \beta b_2$, which with Eq. 3 gives:

$$b_2 = \sqrt{\frac{4M_y}{(1+\beta)df_{h,t}\beta}} \quad (4)$$

The shear capacity of the connection can be written as,

$$R = \beta f_{h,t} d b_2 \quad (5)$$

which gives:

$$R = \sqrt{\frac{4M_y f_{h,t} d\beta}{(1+\beta)}} \tag{6-a}$$

In Fig 1 b), the shear capacity of the connection can be written as,

$$R = \frac{f_{h,t} d(l-p)}{1+\beta}\left(\sqrt{\beta + 2\beta^2\left(1+\frac{p}{l-p}+\left(\frac{p}{l-p}\right)^2\right)+\beta^3\left(\frac{p}{l-p}\right)^2} - \beta\left(1+\frac{p}{l-p}\right)\right) \tag{6-b}$$

where l = the total length of bolt, and p = penetration depth of bolt in concrete. In Fig 1 c), the shear capacity of the connection can be written as,

$$R = \frac{f_{h,t} dp}{2+\beta}\left(\sqrt{\frac{4M_y\beta^2(2+\beta)}{f_{h,t}p^2 d} + 2\beta(1+\beta)} - \beta\right) \tag{6-c}$$

where $\beta = \frac{f_{h,t}}{f_{h,c}}$, a_1, a_2, b_1 are presented in Fig. 1 c).

In the mechanical model stated previously, the withdrawal force and frictional force were not taken into account because they were very low. Therefore, Eq. 6 is a conservative estimate value for the shear capacity of bolt-type connectors in TCC structures.

According to standard EN 1995-1-1 (2014) for bolts and laminated veneer lumber (LVL), the embedment strength was conservatively estimated by Eq. 7, and the characteristic value for the yield moment was estimated by Eq. 8 according to Blass *et al.* (2001).

$$f_{h,t} = 0.082(1-0.01d)\rho_k \tag{7}$$

where ρ_k is the characteristic timber density, in kg/m^3,

$$M_y = 0.3 f_u d^{2.6} \tag{8}$$

where f_u is the characteristic tensile strength of the bolt in N/mm^2.

Because the bolts fail in the concrete when the composite structure reaches its ultimate capacity, information about the embedment strength of the concrete is needed. The embedment strength is assumed to be,

$$f_{h,c} = \frac{P_u}{dh} \tag{9}$$

where d is the diameter of the bolt, h is the total length in concrete block including the head length of the bolt, and the P_u is the shear force resistance of bolt in a concrete encasement, which is assumed according to Eq. 6.19 in Eurocode 4 (EN 1994-1-1 2004). The shear forces resistance is given by,

$$P_u = 0.29 d^2 \sqrt{f_{ck} E_{cm}} \qquad \text{for } h/d > 4 \tag{10}$$

where d is the diameter of the bolt, f_{ck} is the characteristic cylinder compressive strength of the concrete, and E_{cm} is the mean secant modulus of elasticity of concrete.

Then, Eqs. 7 through 10 were substituted into Eq. (6), such that the capacity of bolt-type connector is written as,

$$\sqrt{\frac{7.305 f_u d^{3.6} \rho_k (1-0.01d)\sqrt{f_{ck} E_{cm}}}{0.082\rho_k dh(1-0.01d) + 74.24\sqrt{f_{ck} E_{cm}}}} \quad a)$$

$$R = \frac{f_{h,t} d(l-p)}{1+\beta}\left(\sqrt{\beta + 2\beta^2\left(1+\frac{p}{l-p}+\left(\frac{p}{l-p}\right)^2\right)+\beta^3\left(\frac{p}{l-p}\right)^2} - \beta\left(1+\frac{p}{l-p}\right)\right) \quad b)$$

$$\frac{f_{h,t} dp}{2+\beta}\left(\sqrt{\frac{1.2 f_u d^{2.6}\beta^2(2+\beta)}{f_{h,t} p^2 d} + 2\beta(1+\beta)} - \beta\right) \quad c) \quad (11)$$

where R is the shear capacity in N, the other variables are the same as aforementioned, in Eq. 11 b) and c), β is a parameter which can be written as,

$$\beta = \frac{0.29 d^2 \sqrt{f_{ck} E_{cm}}}{0.082 dh\rho_k (1-0.01d)} \quad (12)$$

Materials

Timber

Xing'an larch is a hardwood that is appropriate for engineering applications. The xing'an larch wood used in these experiments was grown in the forest of the Great Khingan Mountains of China, and was bought from a furniture factory in Central South University of Forestry and Technology, Changsha, Hunan, China. All glued timber blocks used in the tests were made of the larch wood and glued with polyurethane.

According to the standard method for testing mechanical properties of timber structures (GB/T 50708 2012), three full scale specimens with dimensions of 200 mm × 120 mm × 400 mm were tested (Fig. 2), and the compressive strength was by tests found to be 44.9 MPa.

Fig. 2. Compressive strength full scale tests of timber

Before the push-out experiments, the density of timber was determined with six specimens with dimensions of 20 mm × 20 mm × 20 mm. The mean density of timber was found to be 552.1 kg/m^3.

The aqueous polyurethane adhesive was purchased from Nanjing Skybamboo Science and Technology Industry Co., Ltd., Nanjing, China. The shear strength of this adhesive is equal to or greater than 10 MPa for hardwood and equal to or greater than 6 MPa for softwood, with wood failure ratio of 60% and 65%, respectively.

Concrete

All concrete blocks were made in the laboratory of Central South University of Forestry and Technology. The cement with strength grade of 42.5, sand, and gravel were bought from a local building materials factory in Changsha, China. The expected strength class of concrete was C45. The actual mean strength of the concrete was by tests found to be 49.70 MPa (Fig. 3). For specimen D12L120-3, the concrete was cast without vibration by mistake.

Fig. 3. Compressive strength tests of concrete

Steel

The bolts had M-threading and were bought from Suzhou Qiangda Fastener Industry Co., Ltd., Suzhou, China. The bolt tensile strength was 1200 MPa, and the yield strength was 1080 MPa.

Design of Push-out Specimens

Push-out specimens consisted of two sides of concrete and one timber block with dimensions according to Fig. 4. After cutting and drilling a hole in the timber and before pouring the concrete, bolts with various parameters (Table 1) were driven into the timber without twist.

Table 1. Dimensions of Bolts

No.	Bolt		Penetration Depth in Timber, p (mm)
	Diameter (mm)	Length (mm)	
D8L120	8	120	80
D12L120	12	120	80
D16L120	16	120	80
D16L100	16	100	60
Note: the length of bolt does not include the head, which is 10 mm long.			

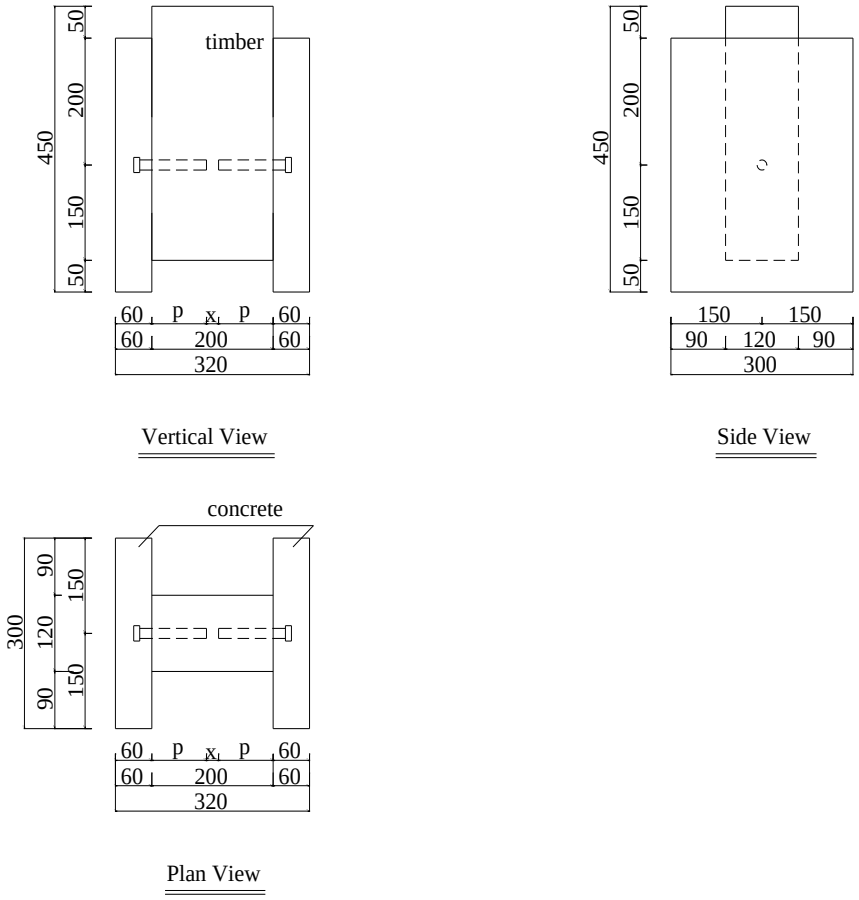

Fig. 4. Drawings of timber-concrete composite push-out specimens (in mm)

Test Methods

The standard BS EN 26891 (BS EN 26891 1991) was followed for the statically loaded tests of TCC specimens. The loading procedure was followed according to Fig. 5.

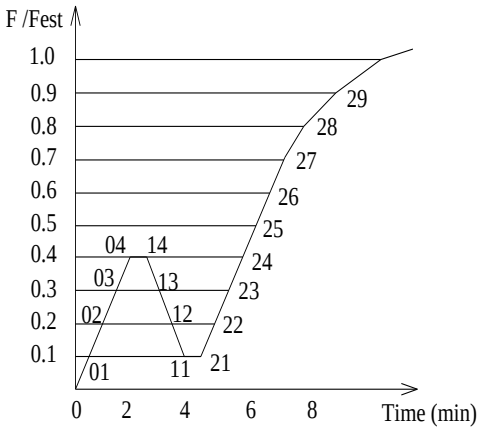

Fig. 5. Load procedure for tests according to EN 26891

The test was conducted with a preliminary test and main test. In the preliminary process, the load, F, was applied up to 0.4 F_{est} and maintained for 30 s, F_{est} being the estimated failure load. Subsequently, the load was lowered to 0.1 F_{est} and maintained for 30 s. In the main test process, the test was conducted under load control until 0.4 F_{est}, followed by displacement control until 15 mm or structure failure.

A universal testing machine (WEW-100, Shenzhen SANS Materials Testing Co., Ltd., Shenzhen, China) was used to apply load to the top surface of the timber in TCC specimens. Four displacement gauges were used to measure the interlamination slip between the concrete and the timber (Fig. 6).

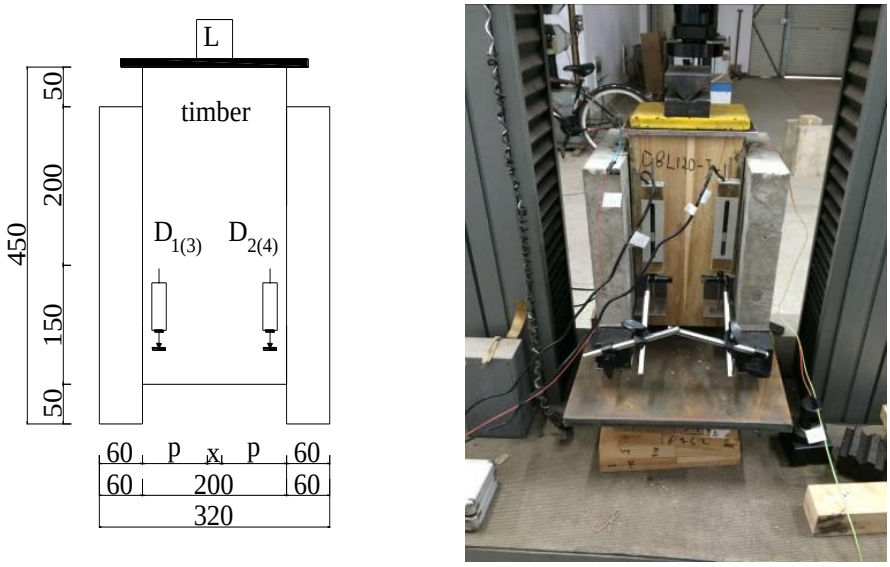

Fig. 6. Testing apparatus

RESULTS AND DISCUSSION

Load-slip curves for all series of specimens are presented here, together with the ultimate load (F_{max}), initial slip (δ), and slip modulus (K_S). The initial slip is the slip corresponding to point 04 in Fig. 5. The slip modulus was calculated with $k_s = 0.4F_{est} / v_{i,\mathrm{mod}}$, where $v_{i,\mathrm{mod}}$ represents modified initial slip, which was calculated with,

$$v_{i,\mathrm{mod}} = \frac{4}{3}(v_{04} - v_{01}) \quad (13)$$

The quantities v_{04} and v_{01} are the slip corresponding to point 04 and 01, respectively. These parameters are usually necessary for the design of the TCC structures (Dias 2005). The initial slip and slip modulus can be calculated according to BS EN 26891 (1991). The mean values, characteristic values and coefficient of variation of the test are presented in Table 2 and Fig. 7. To validate the experimental strength to aforementioned equation, the characteristic values were calculated according to SS EN 14358 (2016).

Table 2. Results for Specimens with Bolt-Type Fasteners

No.	Strength F_{max} (kN)			Initial Slip δ_i (mm)			Slip Modulus K_s (kN/mm)		
	Value	Mean/ Characteristic Value	Cov*	Value	Mean	Cov*	Value	Mean	Cov*
D8L120-1	30.74	27.41/20.50	0.10	1.17	1.67	0.21	11.48	7.55	0.37
D8L120-2	27.54			1.95			6.16		
D8L120-3	23.94			1.88			5.02		
D12L120-1	39.48	39.66/-	0.22	0.88	2.29	0.72	15.22	11.00	0.48
D12L120-2	50.45			1.4			14.29		
D12L120-3	29.03			4.59			3.48		
D16L120-1	58.70	61.29/49.51	0.05	0.77	1.27	0.48	42.55	31.18	0.57
D16L120-2	65.58			0.92			35.76		
D16L120-3	59.59			2.12			15.23		
D16L100-1	54.60	53.01/40.80	0.06	0.695	2.16	0.81	33.09	19.96	0.54
D16L100-2	48.59			4.63			6.88		
D16L100-3	55.84			1.16			19.91		
*Coefficient of variation									

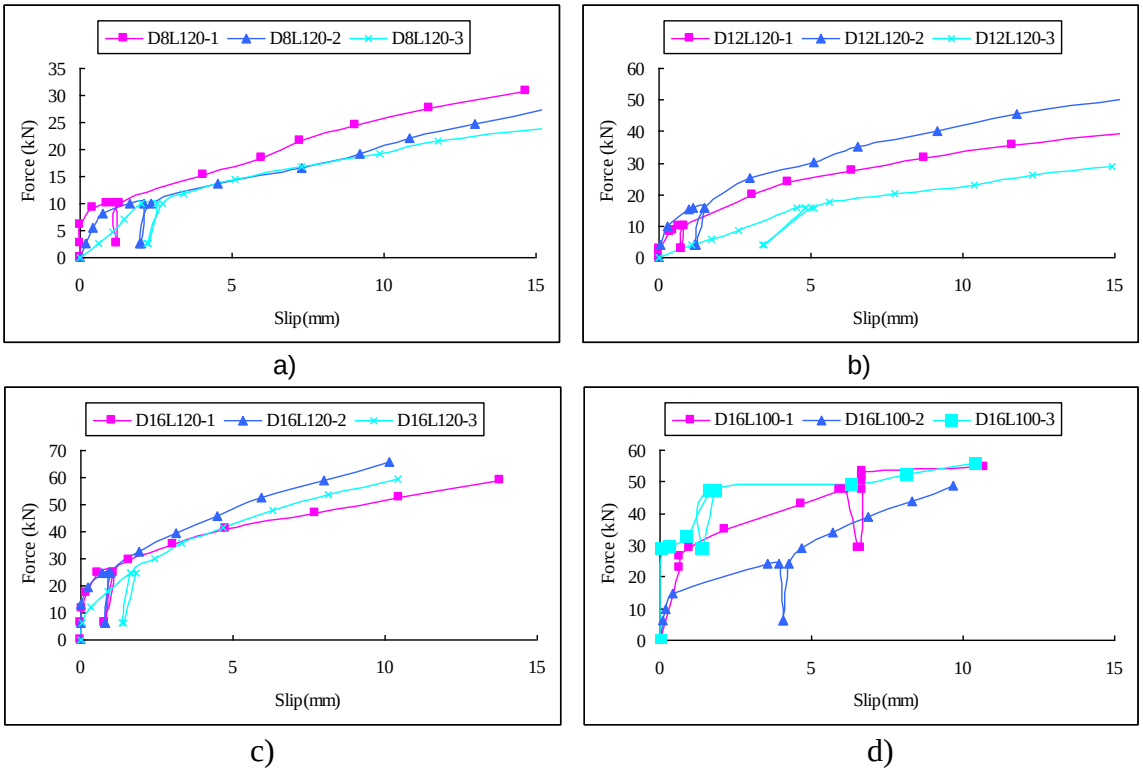

Fig. 7. Load-slip curves for all test groups: a) D8L120, b) D12L120, c) D16L120, and d) D16L100

The mechanical behavior of the bolt-type fasteners showed an obvious non-linear performance for all series. The rate of the interlamination slip between the timber and concrete of all the series of specimens increased with the slip. There was only some minor noise from the timber when the load applied was between 0 to 0.4 times the ultimate estimated load. As the load increased, the slip increased and the noise became louder until the test was completed. When applying load, the timber slowly separated from the concrete. The tests in the D8L120 group and the D12L120 group were stopped when the slip reached 15 mm (BS EN 26891 1991); there was not any obvious material

damage of concrete and timber, except the internal fiber extrusion damage caused by the interlamination slips. The other test finished with a crack in the concrete.

Failure of the three specimens in group D16L100 involved sudden propagation of a transverse horizontal crack in the left or right concrete block. Such cracking was not expected and was most probably due to rotation of the bolt (Fig. 1 c)) and tensile stress in the vicinity of the bolt. For specimen D16L100-1, the cracking load and crack width was 54.59 kN and 2.1mm, respectively. For specimen D16L100-2, the cracking load and crack width was 48.42 kN and 2.5mm, respectively, and for specimen D16L100-3, it was 55.84 kN and 3.5mm, respectively. When the concrete cracked, for specimen D16L100-2 also wood-concrete slip developed, and for specimen D16L100-3 also a diagonal crack developed in the concrete. The bolts in those specimens were found to be rotated. For test group D16L120, there was failure for specimens 1 and 2 due to sudden development of a vertical splitting crack at load 58.70 kN and 48.5 kN, respectively. The vertical crack was caused by tensile stress in the vicinity of the bolt when the bolt rotated. Specimen D16L120-3 failed at load 59.90 kN due to the horizontal type of cracking, for this specimen giving crack width 2.0 mm. The bolts in those specimens were also found to be rotated.

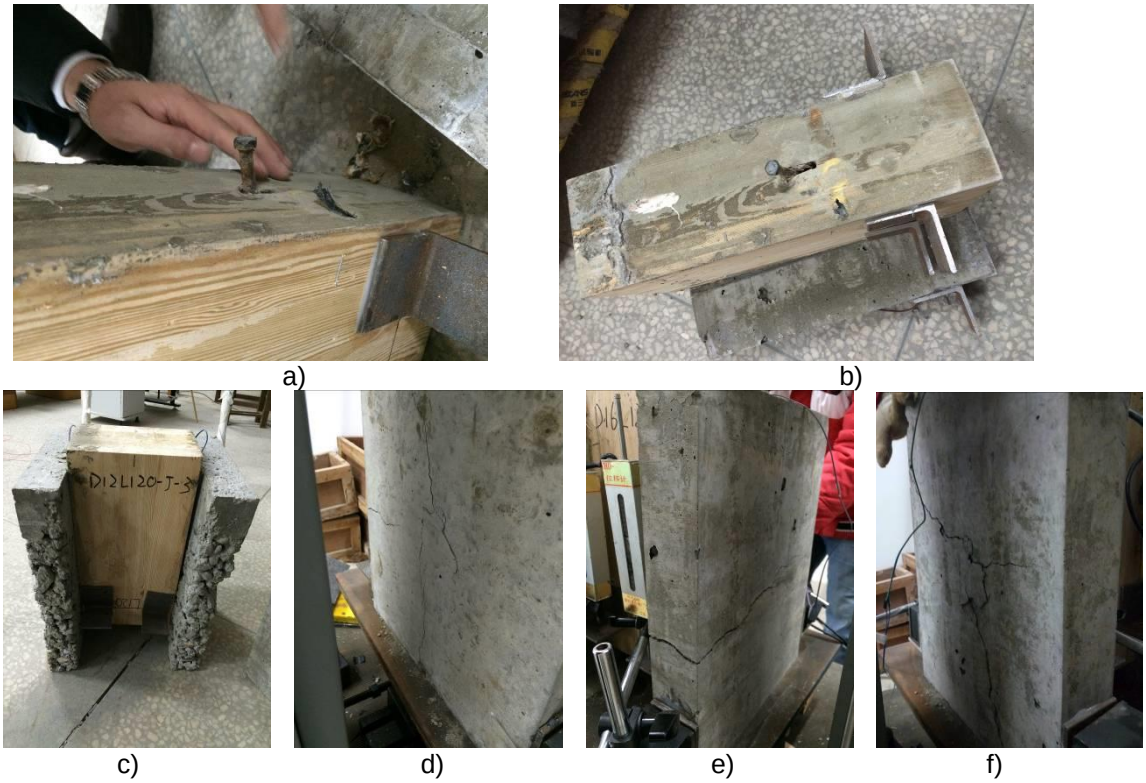

Fig. 8. Failure modes for timber-concrete composite specimens with bolt: a) bolt bended and failed, b) Slip on timber, c) concrete separated from timber, d) vertical crack, e) transverse crack, and f) Diagonal crack

Influence of Bolt Dimensions

Table 3 shows the mean values for strength, initial slip, and slip modulus obtained for the 2+3+3 tests D12L120-1, 2, D16L120-1, 2, 3, and D16L100-1, 2, 3 relative to the corresponding mean results of the tests D8L120-1, 2, 3. All these specimens were cast with concrete of the same quality. It seems that the strength is about proportional to the

bolt diameter and the slip modulus is about proportional to the square of the bolt diameter. Decreased bolt length save a slight decrease in strength and a significant decrease in slip modulus.

Table 3. Relative Influence of Bolt Dimensions on Strength, Slip, and Stiffness

D	L	P	Strength	Initial Slip	Slip modulus
8	120	80	1.00	1.00	1.00
12	120	80	1.64	0.68	1.95
16	120	80	2.24	0.76	4.13
16	100	60	1.93	1.30	2.64

Influence of Concrete Strength

The specimen D12L120-3, shown in Fig. 8 c), was cast without vibrating the concrete. This means that the concrete strength for this specimens was lower than for the two specimens D12L120-1, 2. This clearly affected the test performance, see Fig. 7 b). The strength and slip modulus of specimen D12L120-3 were 29.03 kN and 3.48 kN/mm, respectively. The corresponding mean values for the specimens D12L120-1, 2 were 44.97 kN and 14.76 kN/mm, respectively.

Validation of Shear Capacity Equation

With ρ = 562.5 kg/m^3, E_{cm} = 34500 MPa, h = 40 mm, f_{ck} = 0.79×f_{cu} = 0.79× 49.70 = 39.26 MPa and f_u = 1200 MPa, the main experimental and theoretical results are presented in Table 4. The characteristic values were used to validate the equation, but they cannot represent the real strength, because the number of the specimens was too small. The characteristic values for D12L120 were not used to validate because the data for D12L120-3 was unsuccessful. Eq. 11 a) was used to calculate for D8L120, and Eq. 11 b) was used to calculate for D6L120 and D16L100. The comparison of experimental and theoretical results, based on the European yield model, indicated that the capacity equation, based on the failure model, can predict the shear capacity of bolt connections, with an error lower than 25% and 30%, for characteristic value and test mean value respectively.

Table 4. Comparison of Test and Theory Capacity Results

No.	F (kN)	F_t	F_c (kN)	Δ_1 (%)	Δ_2 (%)
D8L120	19.40	27.41	16.69	29.229	-16.23
D12L120	38.25	39.66	-	3.556	-
D16L120	56.20	61.29	49.51	8.308	-13.51
D16L100	50.98	53.01	40.80	3.838	-24.94
Note: F = theory shear capacity based on Eq. 11, F_t = test mean value, F_c = characteristic value, Δ_1 = 100% *(F_t - F) / F_t, Δ_2 = 100% *(F_c - F) / F_c					

The tests mean value of the D8L120 series was a bit larger than the theoretical value. This was attributed to the fact that the connection was in hardening range, and the strength increased after connection yielded. Furthermore, the theory results were conservative, and should take the fraction into consideration. The shear capacity equation can, however, provide conservative results for design.

In addition, the test results of Dias *et al*. (2007) were considered to verify the equation derived in this paper. Both sets of values are presented in Table 5. The

characteristic values were not found in the citation but only the test mean values. These were used to verify the equation, with error lower than 28% for test mean values at 15 mm. Thus, the theoretical shear equation can be used to predict the load capacity of TCC structure.

Table 5. Comparison of Theory Capacity Results and Test Results in Citation

No.	F (kN)	F_5 (kN)	F_{15} (kN)	Δ_1 (%)	Δ_2 (%)
8mm	5.45	5.90	6.80	7.65	19.87
10mmA	9.18	9.60	11.30	4.40	18.78
HSC	10.72	9.70	11.80	-10.53	9.14
MP	9.25	10.50	12.80	11.90	27.73
C	9.48	10.40	13.10	8.80	27.60
LWAC	7.53	7.80	9.30	3.45	19.02
10mmB	16.19	13.80	17.20	-17.32	5.87
INT	16.03	11.70	15.80	-36.97	-1.43
Note: F = theory shear capacity based on Eq. 11, F_5 = test mean value at 5 mm, F_{15} = test mean value at 15 mm, Δ_1 = 100% *(F_5 - F) / F_5, Δ_2 = 100% *(F_{15} - F) / F_{15}					

CONCLUSIONS

1. Three failure modes were studied and the corresponding theoretical capacity equations were provided. The capacity equations are conservative because the friction is not considered.
2. Tests showed that the specimens with bolt diameters 8 mm and 12 mm failed due to development of plastic hinges giving large deformation. The specimens with stiff 16 mm bolts failed due to cracking of the concrete with the rotation of bolt.
3. The shear capacity and the slip modulus of the bolt-type connectors were directly proportional to the diameter of bolts.
4. The theoretical shear capacity equations predicted the load capacity of the TCC structure conservatively and might therefore be useful in practical design of TCC structure.

ACKNOWLEDGMENTS

The authors are grateful for the support of the State Forestry Administration Project 948 (Project No. 2014-4-51), the China National Natural Science Foundation Program (NSFC Project No. 51478485; 51408615), the innovation training base of graduate student in Hunan province (Project No.603-000306) and the Doctoral Innovation Fund of Central South University of Forestry and Technology (Project No. CX2014A07).

REFERENCES CITED

Blass, H. J., Bienhaus, A., and Kramer, V. (2001). "Effective bending capacity of dowel-type fasteners," *Proc., PRO 22, Int. RILEM Symp. on Joints in Timber Structure*s, RILEM Publications S. A. R. L., Cachan Cedex, France, 71-80.

BS EN 26891 (1991). "Timber structures-joints made with mechanical fasteners–general principles for the determination of strength and deformation characteristics," British Standards Institution, London, UK.

Clouston, P., Bathon, L., and Schreyer, A. (2005). "Shear and bending performance of a novel wood-concrete composite system," *Journal of Structural Engineering* 131(9), 1404-1412. DOI: 10.1061/(ASCE)0733-9445(2005)131:9(1404)

Dias, A. M. P. G. (2005). *Mechanical Behavior of Timber-Concrete Joints*, Ph.D. dissertation, Universidade de Coimbra, Coimbra, Portugal.

Dias, A. M. P. G., Lopes, S. M. R., Van de Kuilen, J. W. G., and Cruz, H. M. P. (2007). "Load-carrying capacity of timber–concrete joints with dowel-type fasteners," *Journal of Structural Engineering* 133(5), 720-727. DOI: 10.1061/(ASCE) 0733-9445 (2007) 133:5(720)

Dias, A. M. P. G., Cruz, H. M. P., Lopes, S. M. R., and Van de Kuilen, J. W. (2010). "Stiffness of dowel-type fasteners in timber–concrete joints," *Structures and Buildings* 163(SB4), 257-266. DOI: 10.1680/stbu.2010.163.4.257

EN 1994-1-1 (2004). "Eurocode 4: Design of composite steel and concrete structures – Part 1-1: General rules and rules for buildings," European Committee for Standardization, Brussels, Belgium.

EN 1995-1-1 (2014). "Eurocode 5: Design of timber structures - Part 1-1: General - Common rules and rules for buildings," European Committee for Standardization, Brussels, Belgium.

GB/T 50708 (2012). "Technical code of glued laminated timber structures," Chinese Ministry of Construction, Beijing, China.

Grantham, R., Enjily, V., Fragiacomo, M., Nogarol, C., Zidaric, I., and Amadio, C. (2004). "Potential upgrade of timber frame buildings in the UK using timber-concrete composites," in: *Proceedings of the 8th World Conference on Timber Engineering, Vol. 2*, Lathi, Finland, pp. 59-64.

Johansen, K. W. (1962). *Yield-line Theory*, Cement and Concrete Association, London, UK.

Li, Z., Xiao, Y., Wang, R., and Monti, G. (2014). "Studies of nail connectors used in wood frame shear walls with ply-bamboo sheathing panels," *Journal of Materials in Civil Engineering* 27(7). DOI: 10.1061/(ASCE)MT.1943-5533.0001167

Lukaszewska, E. (2009). *Development of Prefabricated Timber-Concrete Composite Floors*, Ph. D. thesis, Luleå University of Technology, Luleå, Sweden.

Mascia, N. T., and Soriano, J. (2004). "Benefits of timber-concrete composite action in rural bridges," *Materials and Structures* 37(2), 122-128. DOI: 10.1007/BF02486608

Natterer, J., Hamm, J., and Favre, P. (1996). "Composite wood-concrete floors for multi-story buildings," in: *Proceedings of the International Wood Engineering Conference, Vol. 3*, New Orleans, USA, pp. 431-435.

Rodrigues, J. N., Dias, A. M. P. G., and Providência, P. (2013). "Timber-concrete composite bridges: State-of-the-art review," *BioResources* 8(4), 6630-6649. DOI: 10.15376/biores.8.4.6630-6649

Skinner, J., Bregulla, J., Harris, R., Paine, K., and Walker, P. (2014). "Screw connectors for thin topping, timber-concrete composites," *Materials and Structures* 47(11), 1891-1899. DOI: 10.1617/s11527-013-0158-6

SS EN 14358 (2016). "Timber structures – Calculation and verification of characteristic values," Swedish Standards Institute, Stockholm, Sweden.

Van de Kuilen, J. W. G., and Dias, A. M. P. G. (2011). "Long-term load–deformation behaviour of timber–concrete joints," *Structures and Buildings* 164(SB2), 143-154. DOI: 10.1680/stbu.10.00021

Yeoh, D., Fragiacomo, M., de Franceschi, M., and Boon, K. H. (2011). "State of the art on timber-concrete composite structures: Literature review," *Journal of Structural Engineering* 137(10), 1085-1095. DOI: 10.1061/(ASCE)ST.1943-541X.0000353

Article submitted: April 25, 2016; Peer review completed: July 30, 2016; Revised version received: August 20, 2016; Further revised version received and accepted: August 30, 2016; Published: September 13, 2016.
DOI: 10.15376/biores.11.4.9205-9218